Contrib Mineral Petrol (2012) 163:449–465
DOI 10.1007/s00410-011-0683-7

ORIGINAL PAPER

Magma accumulation rates and thermal histories of plutons of the Sierra Nevada batholith, CA

Jesse W. Davis · Drew S. Coleman · John T. Gracely · Richard Gaschnig · Michael Stearns

Received: 19 February 2011 / Accepted: 13 August 2011 / Published online: 31 August 2011

Abstract Zircon U–Pb geochronology results indicate that the John Muir Intrusive Suite of the central Sierra Nevada batholith, California, was assembled over a period of at least 12 Ma between 96 and 84 Ma. Bulk mineral thermochronology (U–Pb zircon and titanite, $^{40}Ar/^{39}Ar$ hornblende and biotite) of rocks from multiple plutons comprising the Muir suite indicates rapid cooling through titanite and hornblende closure following intrusion and subsequent slow cooling through biotite closure. Assembly of intrusive suites in the Sierra Nevada and elsewhere over millions of years favors growth by incremental intrusion. Estimated long-term pluton assembly rates for the John Muir Intrusive Suite are on the order of 0.001 $km^3\ a^{-1}$ which is inconsistent with the rapid magma fluxes that are necessary to form large-volume magma chambers capable of producing caldera-forming eruptions. If large shallow crustal magma chambers do not typically develop during assembly of large zoned intrusive suites, it is doubtful that the intrusive suites represent cumulates left behind following caldera-forming eruptions.

Keywords Geochronology · Thermochronology · Pluton · Pluton emplacement · Sierra Nevada batholith

Communicated by J. Blundy.

Electronic supplementary material The online version of this article (doi:10.1007/s00410-011-0683-7) contains supplementary material, which is available to authorized users.

J. W. Davis (✉) · D. S. Coleman
Department of Geological Sciences, University of North Carolina at Chapel Hill, 104 South Road, Mitchell Hall, Chapel Hill, NC 27599, USA
e-mail: jesse.w.davis@exxonmobil.com

Present Address:
J. W. Davis
ExxonMobil Production Company,
396 West Greens Road, Houston, TX 77067, USA

J. T. Gracely
ExxonMobil Exploration Company,
P.O. Box 4778, Houston, TX 77060, USA

R. Gaschnig
School of Earth and Environmental Sciences, Washington State University, Webster Physical Science Building, Pullman, WA 99164, USA

M. Stearns
Department of Earth Science, University of California, Webb Hall, Santa Barbara, CA 93106, USA

Introduction

During the Mesozoic, the western boundary of North America was an active continental magmatic arc. The Sierra Nevada batholith, a dominant feature of the Cordilleran of the western United States, was assembled during subduction of an oceanic plate beneath continental North America. Today, the Sierra Nevada is exposed as a mountain range that includes some of the highest topography in the contiguous United States.

The processes by which plutons amalgamate into batholiths and are subsequently exhumed are important to understanding continental crustal growth. Exposures of Sierra Nevada batholithic rocks are the result of dynamic processes that occurred at various crustal levels over hundreds of millions years. Fundamentally, pluton assembly and batholith development are tectonic issues because they are controlled by the ability of tectonic processes to produce magmas and the ability of the lithosphere to make space to accommodate these magmas. Although significant

research has focused on the timescales and mechanisms by which batholiths grow, controversy remains. At the center of this controversy is understanding the rates at which plutons are assembled, and the control that assembly rates have over the ability to sustain shallow crustal magma bodies with significant (>50%) proportions of liquid (Jellinek and DePaolo 2003; Glazner et al. 2004; Lipman 2007).

Models for caldera collapse and associated ignimbrite eruptions (Lipman 2007) have led to the view that plutons represent the remains of large-volume magma chambers that are genetically linked to caldera-forming eruptions (Hildreth 2004; Bachmann et al. 2007). In contrast, recent studies indicate that some plutonic suites were emplaced incrementally through amalgamation of intrusions over millions of years and consequently were not formed by the crystallization of large-volume magma chambers (Coleman et al. 2004; Glazner et al. 2004). Seismic data are consistent with the long timescale of plutonic suite construction because geophysical studies have failed to locate large volumes of melt beneath active volcanic regions (Iyer 1984; Waite and Moran 2009; Chu et al. 2010).

Detailed field mapping, geochronology, thermochronology, and thermal modeling can be used to test competing hypotheses for pluton assembly processes and links between zoned intrusive suites and eruption of highly evolved magmas. Detailed mapping can be used to elucidate pluton emplacement mechanisms. By combining field mapping with detailed geochronology, magma fluxes during pluton assembly can be calculated. Finally, thermochronologic data and modeling can be used to evaluate whether large-volume magma chambers were sustained during pluton assembly.

In order to investigate the development of zoned intrusive suites, the crystallization ages and thermal histories (approximately 750–300°C) are determined for multiple plutons in the central Sierra Nevada batholith of California. The zoned Cretaceous intrusive suites of the Sierra Nevada provide an opportunity to examine the magma fluxes and thermal histories of the large zoned suites that are conceptually linked to silicic ignimbrite eruptions (e.g., Hildreth 2004; Lipman 2007).

The John Muir Intrusive Suite (hereafter referred to as the Muir suite) is chosen as a study area because it provides excellent exposure of rock-types that contain minerals useful for quantifying thermal histories (zircon, titanite, hornblende, and biotite). Furthermore, the intrusive suite is thoroughly mapped at large scale (Moore 1963; Bateman et al. 1964; Bateman 1965; Bateman et al. 1965; Bateman and Dodge 1970; Lockwood and Lydon 1975; Frost and Mahood 1987; Bateman 1992), and some areas are well mapped at much smaller scale (Hathaway 2002; Mahan et al. 2003; Stearns and Bartley 2010). The following methodologies are conducted to meet the study's objectives:

- Detailed field mapping of the southern Lamarck Granodiorite in the Dusy Basin area is conducted to investigate pluton emplacement mechanisms
- Zircon U–Pb geochronology is combined with existing geologic mapping to determine long-term magma fluxes during the growth of the Muir suite
- Zircon U–Pb geochronology is combined with U–Pb titanite ages and $^{40}Ar/^{39}Ar$ thermochronology to evaluate the crystallization and thermal histories (T-t) of the Muir suite

Geologic background

The geology of east-central California is dominated by the Sierra Nevada batholith. The batholith includes over 40,000 km^2 of exposed plutonic rocks and extends approximately 600 km along the western edge of the North American craton (Kistler 1990; Bateman 1992). The majority of the exposed Sierra Nevada batholith intruded at depths around 4–15 km (Ague and Brimhall 1988). Batholithic rocks range in composition from gabbro to leucogranite, with tonalite, granodiorite, and granite being the most abundant (Bateman 1992). Most plutons were emplaced during three major magmatic episodes: 225–195 Ma, 180–165 Ma, and 102–85 Ma (Stern et al. 1981; Chen and Moore 1982; Frost and Mattinson 1993; Saleeby et al. 1990, 2008; Coleman and Glazner 1998; Coleman et al. 2004).

In the eastern Sierra Nevada, the latest magmatic episode is characterized by intrusion of closely related plutons with similar composition, texture, fabric, age, and emplacement depth that Bateman (1992) assigned to different intrusive suites (Fig. 1 inset). From north to south, these include the Tuolumne, Muir, and Whitney intrusive suites. There is also an informally named suite north of the Tuolumne Intrusive Suite (the Sonora pluton [Kistler et al. 1986]) and the Domelands Intrusive Suite (Saleeby et al. 2008) south of the Whitney suite.

The Muir suite (as originally defined) includes (from approximately W to E) the Mount Givens pluton, the Evolution Basin Alaskite, the Lamarck Granodiorite, the Lake Edison Granodiorite, the Mono Creek Granite and the Round Valley Peak Granodiorite (Fig. 1; Bateman and Dodge 1970). The Mt. Givens pluton is excluded from discussion of the Muir suite here because the pluton and Muir suite are separated by a large mass of Jurassic and older rocks. The Evolution Basin Alaskite was also included with the Muir suite; however, portions of what were mapped as Evolution Basin Alaskite were recently reassigned to the Lamarck Granodiorite on the basis of

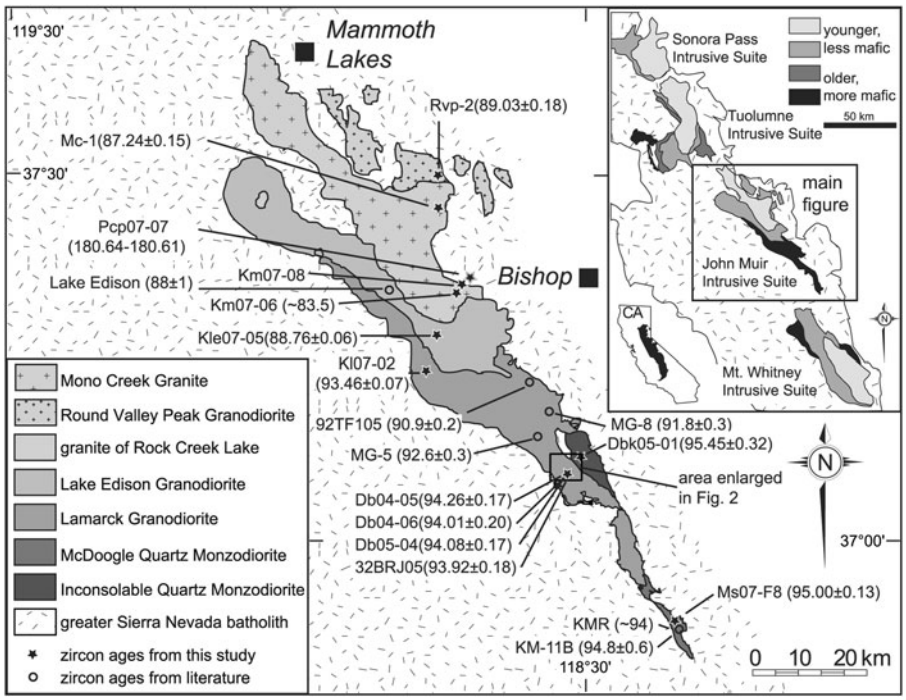

Fig. 1 Simplified geologic map of the John Muir Intrusive Suite after Bateman (1992). Figure shows the nomenclature and approximate locations of samples analyzed in this study and several from the literature. Ages shown are determined from U–Pb zircon isotope data and are reported in millions of years. The errors are reported at 2-sigma uncertainty. Lamarck Granodiorite (92TF105, MG-8, MG-5) ages are from Coleman et al. (1995). Lake Edison age is from Tobisch et al. (1995). McDoogle Quartz Monzodiorite (KMR, KM-11B) ages are from Mahan et al. (2003). *Black box* indicates location of the Dusy Basin region that is expanded in Fig. 2. Inset: zoned intrusive suites that are associated with the Cretaceous Sierra Crest magmatic event (Coleman and Glazner 1998). Outcrop pattern after Bateman (1992) and Tikoff and Teyssier (1992)

field relations (Gracely 2006). Furthermore, preliminary zircon U–Pb geochronology from the western portion of the Evolution Basin Alaskite suggests a crystallization age of approximately 150 Ma (J. Wenner, unpublished data). Consequently, we suspect that the Evolution pluton is composite with a Jurassic portion to the west and a Cretaceous portion that we include with the discussion of the Lamarck Granodiorite. Although we exclude the Mt. Givens pluton and part of the Evolution pluton from discussion of the Muir suite, zircon U–Pb geochronology (Mahan et al. 2003; this study) and field relationships (Mahan et al. 2003; Gracely 2006; this study) suggest that the Inconsolable Quartz Monzodiorite and the McDoogle Quartz Monzodiorite should be included in the Muir suite (Fig. 1).

All of the plutons in the Muir suite have elongate map patterns (Fig. 1). However, plutons exposed in the northern portion of the suite (including the northern Lamarck Granodiorite, Lake Edison Granodiorite, Mono Creek Granite, and the Round Valley Peak Granodiorite) have ages, textures, and compositional variations that mimic those of concentrically zoned, nested intrusions, such as the Tuolumne and Mount Whitney intrusive suites (Fig. 1; Bateman 1992; Hirt 2007). Geobarometry data suggest that the exposed surface of the Muir suite crystallized at depths between 8–12 km (Ague and Brimhall 1988).

Several studies present zircon U–Pb isotope data that define a Late Cretaceous age-span for the Muir suite plutons. Stern et al. (1981) contributed a significant amount of age data throughout the Muir suite including discordant ages of 89.8 Ma and 93.2 Ma for the Lake Edison Granodiorite, a discordant age of 89.6 Ma for the Lamarck Granodiorite, a discordant age of 88.4 Ma for the Mono Creek Granite, a concordant age of 75.8 Ma for the Mono Creek Granite, and a discordant age of 89.1 Ma for the Round Valley Peak Granodiorite. Coleman et al. (1995) presented several concordant zircon ages for rocks from to the Lamarck Granodiorite, suggesting multiple intrusions of approximately 92 Ma. Mahan et al. (2003) obtained ages of 94 Ma from the central phase of the McDoogle Quartz Monzodiorite and 94.8 Ma from the McDoogle's border phase. Tobisch et al. (1995) determined an age of 88 Ma for the Lake Edison Granodiorite. Other studies focused on the dating mafic plutons in the vicinity of the Muir suite. Frost and Mattinson (1988) determined a discordant age of 97.5 Ma for the quartz diorite of Pine Lake. Gaschnig (2005) presented an age of 95.0 Ma for the Rock Creek Gabbro.

Methods

Field work

Detailed geologic mapping was conducted in the Dusy Basin area of the Lamarck Granodiorite in order to obtain samples for geochronology with well-documented field relations. Mapping focused on: (1) determining petrographic variations of the Lamarck Granodiorite and Inconsolable Quartz Monzodiorite, including determining variations in composition, color index, phenocryst abundance, enclave aspect ratios and abundance, and foliation type; (2) identification of internal contacts within the Lamarck Granodiorite; and (3) establishing relative age relationships between units flanking the Lamarck Granodiorite and units internal to the Lamarck Granodiorite.

U–Pb analyses

Zircon and titanite separates were obtained by mechanical disaggregation (jaw crusher and disk mill), water table, heavy liquids, and magnetic separator techniques. Zircon grains were thermally annealed and subjected to chemical abrasion in order to eliminate volumes affected by radiation damage and to remove any inclusions (Mundil et al. 2004; Mattinson 2005). Zircon and titanite fractions were spiked using a ^{205}Pb-^{233}U-^{236}U tracer (Parrish and Krogh 1987) and dissolved following a procedure modified after Krogh (1973) and Parrish (1987). Uranium and Pb were isolated using HCl (zircon) and two-stage HBr-HCl (titanite) anion exchange column chromatography procedures modified after Krogh (1973). Isotope ratios of both U and Pb were determined by thermal ionization mass spectrometry (TIMS) on the VG Sector 54 mass spectrometer at the University of North Carolina at Chapel Hill (Online Resource 1). Uranium was run as a metal after loading in graphite and H_3PO_4 on single Re filaments. Lead was loaded in silica gel on single Re filaments. All data were collected using the Daly detector in peak switching mode. Mass fractionation for Pb was determined to be 0.15%/a.m.u (atomic mass unit) over a wide temperature range based on multiple analyses of the NBS-981 common Pb standard. Mass fractionation for U was calculated in real time using the ^{233}U/^{236}U ratio (a known constant from the ^{205}Pb-^{233}U-^{236}U tracer) and assuming linear fractionation. Data processing and age calculations were completed using the algorithms of Ludwig (1980, 1998) and Isoplot v. 3.00 (Ludwig 2003). Decay constants used were $^{238}\mathrm{U} = 0.155125 \times 10^{-9} \pm 0.16598 \times 10^{-14}$ a^{-1}, and $^{235}\mathrm{U} = 0.98485 \times 10^{-9} \pm 0.13394 \times 10^{-13}$ a^{-1} (Jaffey et al. 1971; Steiger and Jäger 1977). All errors are reported at 2-sigma uncertainty and consider analytical and decay-constant uncertainties.

Titanite common Pb correction

To help minimize uncertainty in the common Pb correction for titanite samples, the composition of the common Pb was determined from leached K-feldspar grains. K-feldspars were separated using the same procedures as for zircon and titanite. Milligram-sized fractions of hand-picked K-feldspar grains were progressively leached following the methods of Schmitz (2010). Residue and all leachates were dried and redissolved in HBr for separation of Pb by HBr-HCl anion exchange column chromatography. Separated Pb was analyzed by thermal ionization mass spectrometry (TIMS) on the VG Sector 54 mass spectrometer at the University of North Carolina at Chapel Hill in static multicollector mode using faraday detectors. Mass fractionation for Pb in multicollector mode was determined to be 0.12%/a.m.u over a wide temperature range based on multiple analyses of the NBS-981 common Pb standard. The isotopic composition of the residue was used as the composition of the common Pb in order to calculate titanite ages (e.g., Schmitz and Bowring 2001; Online Resource 1). Decay constants, data processing, age calculations, and error propagation were completed the same as zircon analyses.

^{40}Ar/^{39}Ar analyses

Hornblende and biotite separates were obtained from the same samples that were used for U–Pb geochronology. Mineral separates were washed, weighed, loaded into Cu-foil, and placed into a machined aluminum disk for irradiation. Separates were analyzed by the incremental-heating method using a double-vacuum molybdenum resistance furnace. Isotope ratios were measured on a MAP-215 50 mass spectrometer at the New Mexico Geochronology Research Laboratory, New Mexico Bureau of Geology (Online Resource 2). Irradiation, instrumentation, and analytical parameters are presented in Online Resources 2.

It is common to report apparent ^{40}Ar/^{39}Ar ages relative to the Fish Canyon sanidine interlaboratory flux monitor (FC-2; 28.02 Ma; Renne et al. 1998) using the $^{40}\mathrm{K}_{\mathrm{total}}$ decay constant of 5.543e^{-10} a^{-1} (Steiger and Jäger 1977). However, Renne et al. (2010) determined a different Fish Canyon sanidine age of 28.305 ± 0.036 Ma as well as different $^{40}\mathrm{K}_{\varepsilon}$ and $^{40}\mathrm{K}_{\beta}$ decay constants of 0.5755 ± 0.0016e^{-10}a^{-1} and 4.9737 ± 0.0093e^{-10} a^{-1}, respectively. Ages for both standard models and decay constants are presented (Table 1); however, the preferred ages are those calculated using Renne et al. (2010).

In composite hornblende grains, fine-grained mica inclusions or fluid infiltration can disturb Ar concentrations and result in complex K/Ca release patterns and anomalously young ages during low-temperature heating steps

Table 1 $^{40}Ar/^{39}Ar$ age comparisons for the John Muir Intrusive Suite

Pluton	Sample ID	Mineral	Age (Ma)[a]	Age (Ma)[b,c]
Inconsolable	Dbk05-01	Hornblende[d]	94.5 ± 0.6	95.4 ± 0.7[f]
Qtz-monzodiorite		Biotite[e]	86.6 ± 0.3	87.5 ± 0.5
Lamarck Granodiorite	Db05-04	Hornblende[d]	93.1 ± 0.4	94.0 ± 0.6
		Biotite[d]	84.8 ± 0.2	85.6 ± 0.4
Lamarck Granodiorite	Db04-05	Biotite[e]	83.2 ± 0.2	84.0 ± 0.4
McDoogle	Ms07-F8	Biotite[d]	83.0 ± 0.2	83.8 ± 0.4
Qtz-monzodiorite				
Lake Edison	Kle07-05	Hornblende[d]	88.2 ± 1.0	89.1 ± 1.1
Granodiorite		Biotite[d]	82.3 ± 0.4	83.1 ± 0.5
Mono Creek Granite	Km07-06	Biotite[e]	81.3 ± 0.2	82.1 ± 0.4
Mono Creek Granite	Km07-08	Biotite[e]	81.3 ± 0.2	82.1 ± 0.4

[a] Ages are calculated using Fish Canyon standard age of Renne et al. (1998) and $\lambda^{40}K_{total}$ of Steiger and Jäger (1977). Errors are reported at 2-sigma uncertainty. Errors incorporate analytical and J-value uncertainties

[b] Ages are calculated using Fish Canyon standard age, $\lambda^{40}K_{\varepsilon}$ and $\lambda^{40}K_{\beta}$ of Renne et al. (2010)

[c] Ages and errors are recalculated using EARTHTIME Ar tool: http://www.earth-time.org/ar-ar.html

[d] Ages from inverse isochrons

[e] Ages from weighted average of all heating steps

[f] Errors are reported at 2-sigma uncertainty. Errors incorporate analytical, J-value, ^{40}K decay constant, and Fish Canyon standard age uncertainties

(Berger 1975; Sisson and Onstott 1986; Miller et al. 1991; Wartho 1995). Heating steps from hornblende separates displaying these complexities were excluded from plateau and isochron determinations and only the intermediate and high-temperature heating steps with uniform K/Ca ratios (near 0.1) were used in determining plateaus and isochrons. Similarly, a decrease in K/Ca ratio for biotite at high-temperature steps indicates degassing of mineral phases other than biotite (Lo and Onstott 1989), and increments that showed this behavior were excluded from plateau and isochron determinations.

Plateau ages were compared to corresponding inverse isochron ages in order to evaluate the impact of excess ^{40}Ar. Overlap of plateau and inverse isochron ages within 2-sigma uncertainty indicates that any excess ^{40}Ar had negligible effect on age determination (e.g., Singer and Pringle 1996).

Thermochronology

Bulk mineral thermochronology was used to determine high-temperature (>300°C) T-t histories by correlating temperatures to ages of coexisting mineral thermochronometers: zircon, titanite, hornblende, and biotite. Titanite, hornblende, and biotite ages indicate the timing when samples passed through respective closure temperatures (Dodson 1973). Diffusion experiments were not conducted during this study. Consequently, estimated closure temperature ranges of 700–660°C for titanite ages (Scott and St-Onge 1995), 580–490°C for hornblende ages (Harrison 1981), and 345–280°C for biotite ages (Harrison et al. 1985) were used.

Results

Field observations

Mapping in Dusy Basin at a scale of 1:10,000 (Fig. 2) reveals nine laterally continuous bodies within the Lamarck Granodiorite and definitive contact relationships of the Lamarck Granodiorite cutting the Inconsolable Quartz Monzodiorite in the northeast. Internal contacts, distinguishable by variations in composition, color index, foliation, and enclave abundance and aspect ratio, are viewable at all scales within the Lamarck Granodiorite in and around Dusy Basin (Fig. 3). Internal contacts are both subtle and obvious, and commonly grade from sharp to gradational to cryptic along strike. Internal contacts have steep dips and strike subparallel to contacts between the Lamarck Granodiorite and adjacent plutons (Fig. 2).

In Dusy Basin, five informal units are distinguished within the Lamarck Granodiorite (Fig. 2; Online Resource 3). A leucocratic granodiorite unit, Kl_1, is characterized by a low color index, high phenocryst abundance, and a mineral-enclave foliation. In addition to continuous bodies that define the eastern and western margins of the Lamarck Granodiorite, isolated bodies of the leucocratic granodiorite occur throughout other units as irregularly shaped screens. An enclave foliated granodiorite unit, Kl_2, is

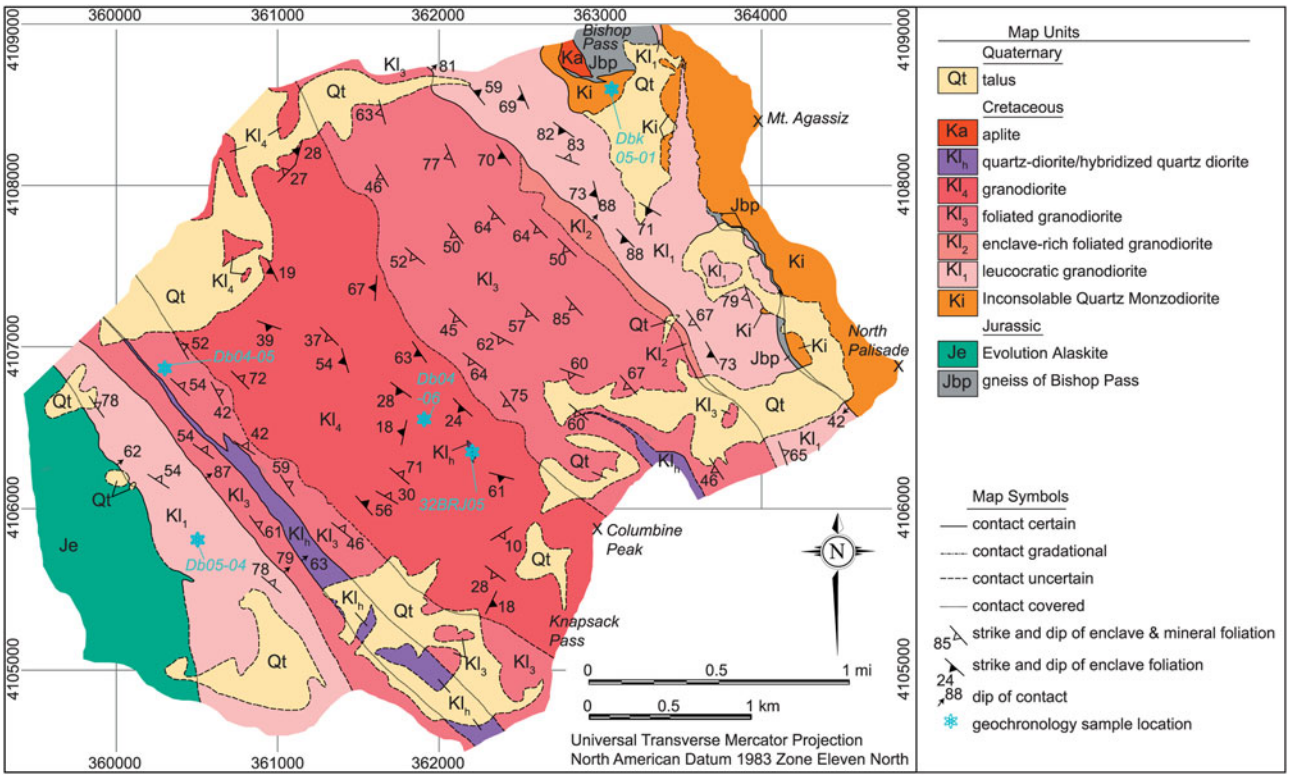

Fig. 2 Geologic map of the Dusy Basin area, central Sierra Nevada batholith, California. The symmetric pattern of map units about the central axis is interpreted as the result of syntaxial incremental intrusion (Bartley et al. 2008) rather than folding (Bateman and Moore 1965) because the foliation is less prevalent in axial units and there is no evidence for regional folding of older rocks

characterized by an intermediate color index, enclave foliation, but no mineral foliation. A mineral-enclave foliated granodiorite unit, Kl_3, has an intermediate color index. A hybridized granodiorite unit, Kl_h, is characterized by an intermediate-to-high color index, which apparently resulted from the hybridization of mafic and intermediate magmas. A weakly foliated granodiorite unit, Kl_4, with an intermediate color index is distinguished by its rounded enclaves, lack of internal contacts, and weak to absent enclave and mineral foliations. Each map unit is characterized by multiple internal contacts that are often laterally continuous for 10's to 100's of meters (Fig. 3). Foliation in these units varies from steep (typically >60°) along the peripheral portions of the pluton to moderately steep (typically 30°–60°) near the center (Fig. 2).

U–Pb Zircon analyses

Zircon fractions from all samples contain few inclusions and lack visible inherited cores. All fractions from the Muir suite are concordant within uncertainty (considering decay-constant and analytical uncertainties; Online Resource 1). Consequently, we report the weighted mean $^{206}Pb/^{238}U$ ages as the interpreted crystallization age of the samples (Fig. 4) with the exception of the Mono Creek Granite sample Km07-06 in which fractions spread significantly; therefore, a weighted mean age is not determined. The quartz diorite of Pine Lake is a wall rock unit of the Muir suite and displays a number of discordant fractions (Online Resource 1).

Samples of the two oldest Muir suite units yield similar ages of 95.45 ± 0.32 Ma (MSWD = 0.6) for the Inconsolable Quartz Monzodiorite and 95.00 ± 0.13 (MSWD = 3.5) for the McDoogle Quartz Monzodiorite (Fig. 4). New ages from the Lamarck Granodiorite range between 94.26 ± 0.17 Ma (MSWD = 1.5) and 93.46 ± 0.07 Ma (MSWD = 0.72) (Fig. 4). Samples collected from the northern Muir suite plutons (Round Valley Peak Granodiorite, Lake Edison Granodiorite, and Mono Creek Granite) are the youngest in the suite and are all younger than 90 Ma (Fig. 4).

U–Pb Titanite analyses

Data for individual titanite fractions are dispersed along a line whose lower intercept with the Tera and Wasserburg (1972) projection of the concordia curve defines the titanite age of the sample (e.g., Ludwig 1998). Titanite ages from the McDoogle Quartz Monzodiorite (Ms07-F8) and a sample from the Lamarck Granodiorite (Db04-05) are

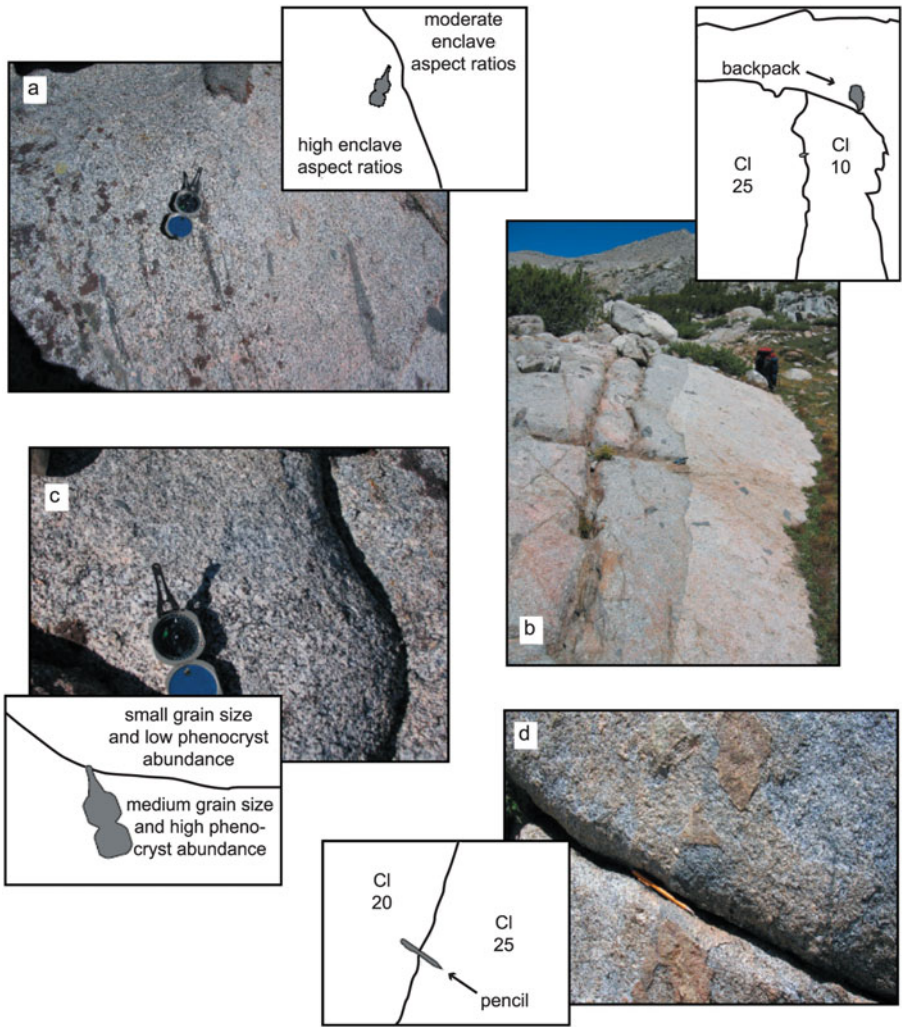

Fig. 3 Internal contacts that are located within the Lamarck Granodiorite. Compasses are oriented to the north. **a** Contact between a unit with high enclave aspect ratios and abundance (*left*) and a unit with moderate enclave aspect ratios and abundance (*right*). **b** A dramatic variation in the color index (CI) defining an internal contact; CI 25 on left and CI 10 on the right. Picture taken looking NW with backpack in the upper right for scale. **c** Subtle variation in grain size and phenocryst abundance; upper unit has a smaller grain size and fewer phenocrysts than the lower unit. **d** Subtle variation in CI delineating an internal contact; CI 20 on the left and CI 25 on the right. The picture is taken looking to the NW with pencil at the center for scale

95.31 ± 0.46 Ma (MSWD = 0.01) and 93.47 ± 0.68 Ma (MSWD = 1.06), respectively (Online Resource 1). Both titanite ages overlap within uncertainty to their corresponding zircon ages (Fig. 4).

^{40}Ar/^{39}Ar analyses

Hornblende

Hornblende samples yield age spectra with a variety of complications (Fig. 5; Online Resource 2). A Lamarck Granodiorite hornblende sample yields a simple age spectrum (Fig. 5b) and a plateau is assigned from contiguous heating steps having apparent ages that overlap within 2-sigma uncertainty. Hornblende samples from the Inconsolable Quartz Monzodiorite and Lake Edison Granodiorite yield age spectra that are characterized by high-temperature heating steps that include very small fractions of the total gas, anomalously young ages, and anomalously high uncertainties (Fig. 5a, c). Hornblende breakdown caused by phase changes during *in vacuo* step heating likely led to high-temperature age spectra complexities (e.g., Wartho et al. 1991). The affected high-temperature heating steps account for less than 4% of the ^{39}Ar released per sample; therefore, noncontiguous heating steps are used when assigning plateaus for these samples.

Hornblendes from the Muir suite have plateau and inverse isochron ages that overlap and thus are interpreted to lack significant excess ^{40}Ar. Generally, inverse isochron ages are more robust than plateau ages (Renne 2006). Consequently, inverse isochron ages are used to evaluate T-t histories (Table 1). Hornblende ages from the Muir suite overlap within uncertainty of their corresponding U–Pb zircon ages (Table 2).

Biotite

The Lamarck Granodiorite, Lake Edison Granodiorite, and McDoogle Quartz Monzodiorite biotites yield simple age spectra (Fig. 6a, b, c; Online Resource 2), and plateaus are determined for all contiguous heating steps with ages that overlap within 2-sigma uncertainty. These biotite samples

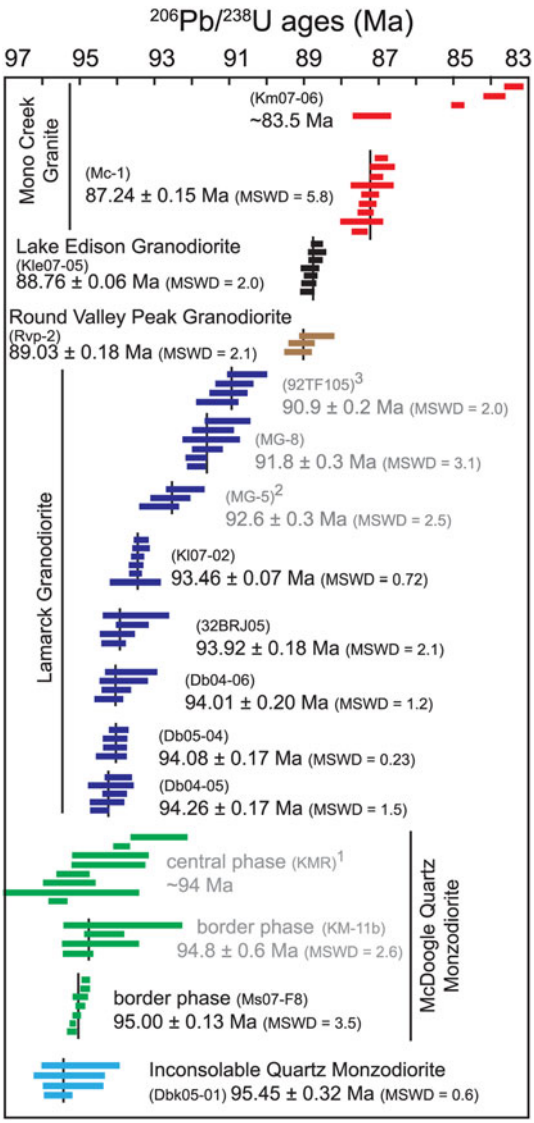

Fig. 4 Compilation of $^{206}Pb/^{238}U$ ages for individual zircon fractions from John Muir Intrusive Suite indicating an intrusive age span ca. 12 Ma. *Errors* are reported at 2-sigma uncertainty and incorporate analytical and decay constant uncertainties of Jaffey et al. (1971). *Black lines* correspond to the sample's $^{206}Pb/^{238}U$ weighted mean age. Samples from this study are shown in *black*, and samples that are from the literature are shown in *grey* {Lamarck Granodiorite: Mt. Gilbert area, Hunchback area, and Lake Sabrina area (Coleman et al. 1995); McDoogle central and border phases (Mahan et al. 2003)}. [1]101 Ma fraction is not included. [2]96.4 Ma fraction is not included. [3]93.4 and 92.4 Ma fractions are not included. Weighted mean ages are calculated using Isoplot v. 3.00 (Ludwig 2003)

do not show excess ^{40}Ar; therefore (as for hornblende ages), inverse isochron ages are used to evaluate their T-t histories (Table 1).

Biotites from the Inconsolable Quartz Monzodiorite and a Lamarck Granodiorite sample yield slightly saddle-shaped age spectra (Fig. 6d, e) that are thought to be caused by ^{39}Ar recoil (e.g., Lo and Onstott 1989). Two Mono Creek Granite biotite samples (Fig. 6f, g) yield slightly hump-shaped age spectra. This pattern suggests that chlorite alteration has affected argon release (Heizler et al. 1988; Sanders et al. 2006). Integrated ages are used to evaluate T-t histories for samples that have saddle or hump-shaped spectra because they lack valid inverse isochrons and do not yield plateaus (Table 1). For all samples, the biotite age postdates the hornblende and zircon ages by several Ma (Table 2).

Discussion

Assembly of the Lamarck Granodiorite in Dusy Basin

Within the Dusy Basin area, relative age relationships between pulses of felsic, intermediate, and mafic phases are well documented by mapping (Fig. 2). The occurrence of isolated leucocratic bodies intruded and partially dissected by the intermediate phase of the Lamarck Granodiorite suggests that the leucocratic phase was the earliest to intrude. Mafic dikes cut foliation and sharp internal contacts within intermediate units, indicating that locally these are the youngest intrusions in the map area. However, preservation of a variety of other mafic magma interactions suggests that mafic magmas intruded throughout the assembly of the Lamarck Granodiorite.

Preservation of map-scale and outcrop-scale internal contacts within Lamarck Granodiorite in the Dusy Basin area is suggestive of pluton assembly by multiple vertical to sub-vertical sheets. Subtle variations in phenocrysts, enclave abundance, and modal mineralogy delineate many internal contacts within the Lamarck Granodiorite. Such variations are typically interpreted to result from in situ evolution owing to mechanical crystal segregation (McBirney and Nicolas 1996) or chemical segregation (McBirney 1995; Boudreau and McBirney 1997). However, neither mechanical segregation indicators (e.g., sharp modal variations, rhythmic grain size layering, grain imbrication) nor chemical segregation indicators (e.g., centimeter to meter scale modal layering) are observed in the study area. Consequently, development of internal contacts through amalgamation of discrete magma pulses is preferred.

Bateman and Moore (1965) first mapped the Lamarck Granodiorite in Dusy Basin as a plutonic synform owing to the steep foliation that dips toward the central part of the basin. Mapping within the Dusy Basin area (Fig. 2) confirms a symmetrical distribution of map units about a central axis and preservation of foliation within marginal units that dips steeply toward the undeformed central unit, reinforcing the observations made by Bateman and Moore (1965). Two hypotheses to account for the map pattern are folding of a sill or dike complex owing to regional shortening (Tikoff and Teyssier 1992; Tikoff and Saint Blanquat

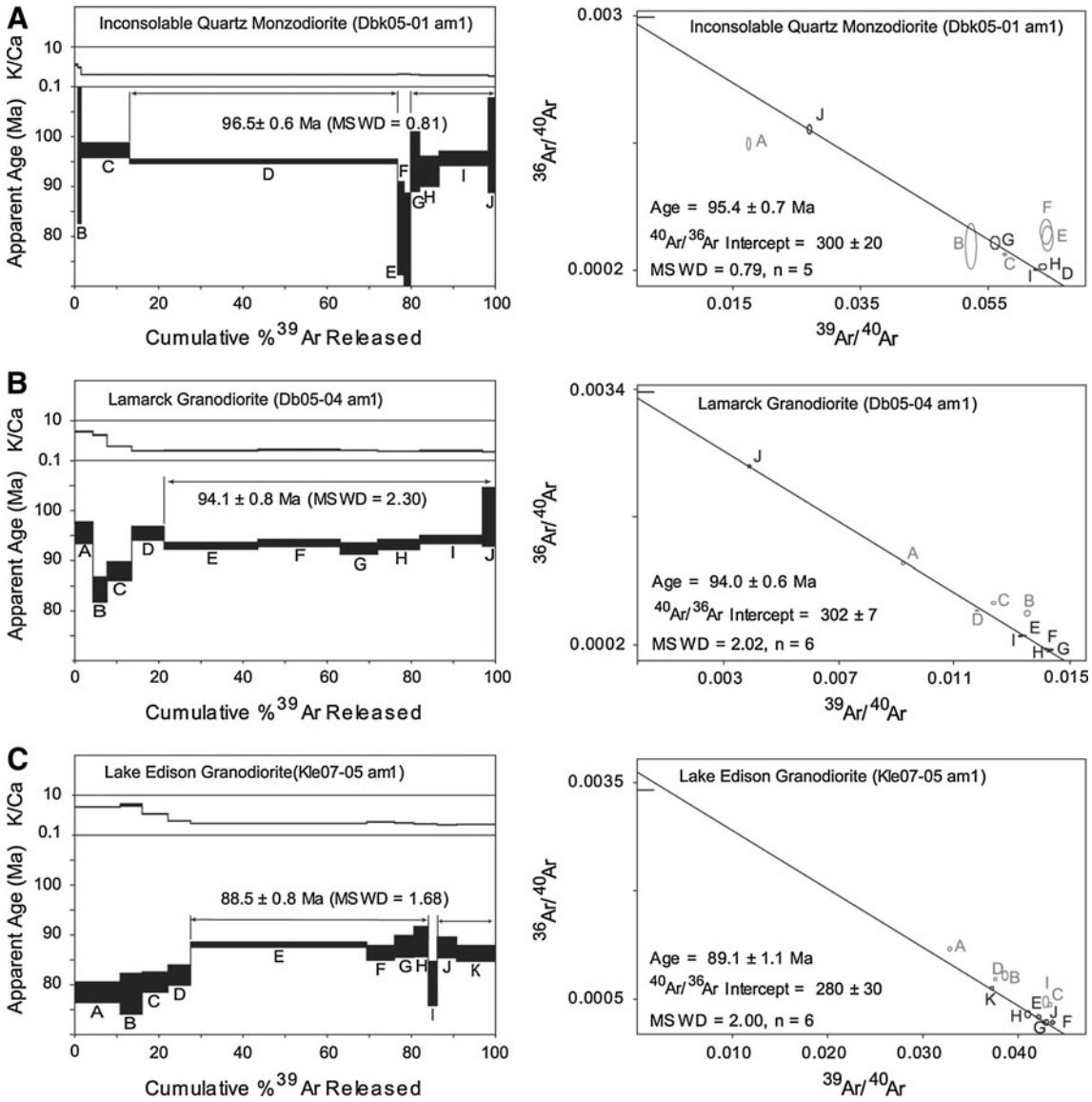

Fig. 5 Hornblende $^{40}Ar/^{39}Ar$ step heating spectra and inverse isochrons from the John Muir Intrusive Suite. Argon ages are calculated using Fish Canyon standard age, $\lambda^{40}K_{\varepsilon}$ and $\lambda^{40}K_{\beta}$ of Renne et al. (2010). Errors incorporate analytical, J-value, ^{40}K decay constant, and Fish Canyon standard age uncertainties. Errors are reported at 2-sigma uncertainty. *Gray* heating steps on inverse isochron are excluded from regressions and age calculations (see text for "Discussion"). The horizontal line on inverse isochrons indicates $^{40}Ar/^{36}Ar = 295.5$

1997) and bilateral symmetry of units resulting from syntaxial crack-seal pluton growth (Bartley et al. 2008).

The lack of a well-defined foliation in the central unit and the absence of axial planar foliation in marginal units preclude the possibility of folding in response to regional shortening. Furthermore, older plutons within the area should have also recorded the shortening event within their fabrics, and there is little evidence to support this (Bateman 1992).

More readily, crack-seal growth of a pluton allows magma to ascend along narrow conduits to emplacement levels resulting in dilation approximately perpendicular to internal contacts (Mahan et al. 2003; Bartley et al. 2008). Syntaxial growth can preserve older units along the margins of the pluton and progressively younger units inward, as is observed within Dusy Basin. Furthermore, the overall elongate outcrop pattern of the Lamarck Granodiorite with internal contacts parallel to its long axis is suggestive of a vertical sheet (dike-like) incremental intrusion emplacement model.

Zircon U–Pb crystallization ages

Most samples from this study yield tightly clustered U–Pb data for which weighted mean $^{206}Pb/^{238}Pb$ ages are calculated, and those ages are accepted as crystallization ages for

Table 2 Compilation of U–Pb and $^{40}Ar/^{39}Ar$ data used to determine T-t histories for the John Muir Intrusive Suite

Pluton	Sample ID	Mineral	Age (Ma)[a,b,c]
Inconsolable	Dbk05-01	Zircon	95.5 ± 0.3
Qtz-monzodiorite		Hornblende	95.4 ± 0.7
		Biotite	87.5 ± 0.5
Lamarck Granodiorite	Db05-04	Zircon	94.1 ± 0.2
		Hornblende	94.0 ± 0.6
		Biotite	85.6 ± 0.4
RLamarck Granodiorite	Db04-05	Zircon	94.3 ± 0.2
		Biotite	84.0 ± 0.4
McDoogle	Ms07-F8	Zircon	95.0 ± 0.1
Qtz-monzodiorite		Titanite	95.3 ± 0.5
		Biotite	83.8 ± 0.4
Lake Edison	Kle07-05	Zircon	88.8 ± 0.1
Granodiorite		Hornblende	89.1 ± 1.1
		Biotite	83.1 ± 0.5
Mono Creek Granite	Km07-06	Zircon	83.5
		Biotite	82.1 ± 0.4
Mono Creek Granite	Km07-08	Biotite	82.1 ± 0.4

[a] Argon ages are calculated using Fish Canyon standard age, $\lambda^{40}K_{\varepsilon}$ and $\lambda^{40}K_{\beta}$ of Renne et al. (2010)

[b] Argon errors are reported at 2-sigma uncertainty. Errors incorporate analytical, J-value, ^{40}K decay constant, and Fish Canyon standard age uncertainties (Renne et al. 2010)

[c] Zircon ages are $^{206}Pb/^{238}U$ weighted mean age of sample. Errors are reported at 2-sigma uncertainty. Errors incorporate analytical and decay constant uncertainty (Jaffey et al. 1971)

the samples. However, several samples yielded data that are either discordant (quartz diorite of Pine Lake Pcp07-07), or concordant, but spread along an interval of concordia and do not overlap within uncertainty (McDoogle Quartz monzodiorite Ms07-F8, Mono Creek Granite Km07-06, Mono Creek Granite Mc-1).

The discordant data are likely the result of Pb-loss. The quartz diorite of Pine Lake (Online Resource 1) was dated as part of this study because earlier work suggested an age (97.5 Ma) similar to the Muir suite (Frost and Mattinson 1988). Zircon fractions from this study for the quartz diorite spread along a discordia line and have $^{206}Pb/^{238}U$ ages ranging from 181 to 132 Ma (Online Resource 1). Two zircon fractions have indistinguishable $^{206}Pb/^{238}U$ ages of 180.6 Ma that is interpreted as the crystallization age. Discordance in the other fractions is attributed to Pb-loss because the quartz diorite is a small body (3 km^2) that is pervasively intruded by sheets of the Late Cretaceous Mono Creek Granite that make up 40% of the outcrop area at Pine Lake where samples for both studies were collected (Frost and Mattinson 1988). The Mono Creek Granite likely contributed enough heat and fluids to disturb zircon systematics. Consequently, the Pine Lake body is interpreted to be Jurassic and the discordant 97.5 Ma age of Frost and Mattinson (1988) to reflect Pb-loss caused by the intrusion of the Muir suite.

The observation that zircon data for individual samples are distributed along an interval of concordia and do not yield ages that overlap within uncertainty is recognized with increasing frequency as the precision of U–Pb data improves (e.g., Miller and Wooden 2004; Miller et al. 2007). The age dispersion along an interval of concordia indicates the potential effects of Pb-loss, grain resorption and regrowth, or extended intervals of zircon crystallization.

Age spread due to Pb-loss is possible in the McDoogle Quartz Monzodiorite (Ms07-F8; Fig. 4) and the Mono Creek Granite (Mc-1, Km07-06; Fig. 4) samples but is not favored here for several reasons. Zircons from the units are not characterized by anomalously high U and Th which can lead to Pb-loss (e.g., Mattinson 2005). In addition, there is nothing unusual about the morphology or the degree of alteration of zircons from these samples in comparison to other samples from this study (and in some cases, from the same unit). There is also no obvious reason why thermal annealing and chemical abrasion of only these samples from the area would not minimize or eliminate Pb-loss.

Miller and Wooden (2004) suggest that zircon U–Pb age dispersion along concordia outside of analytical uncertainty can result from high-temperature fluctuations resulting in zircon resorption and subsequent regrowth in a long-lived magma system. The general observation from this study that U–Pb ages and $^{40}Ar/^{39}Ar$ hornblende ages are concordant for all samples suggest reheating by younger intrusions did not elevate temperatures above hornblende closure (approximately 550°C); however, calculated zircon saturation temperatures (Watson and Harrison 1983) for the samples are 725° ± 25°C. Therefore, it is unlikely that the nearly 4 Ma age dispersion in data from one of the Mono Creek Granite samples (Km07-06; Fig. 4) is caused by zircon grain resorption and regrowth. The McDoogle Quartz Monzodiorite (Ms07-F8; Fig. 4) and a second sample of the Mono Creek Granite (Mc-1; Fig. 4) have much a much smaller spread in ages (approximately 0.5 Ma) which is within the uncertainty of determining concordancy of zircon and hornblende ages. Thus, resorption and regrowth is a plausible explanation for the age dispersion exhibited by these samples.

The large spread in the concordant ages for the Mono Creek Granite sample (Km07-06; Fig. 4) is consistent with prolonged or episodic periods of zircon growth. This pattern of zircon growth is most consistent with the presence of antecrysts grains that were crystallized from earlier pulses of magma that were incorporated into younger magma from the same system (e.g., Miller et al. 2007). This interpretation seems particularly likely in the case of the Mono Creek sample, for which there are nearby dated samples spanning

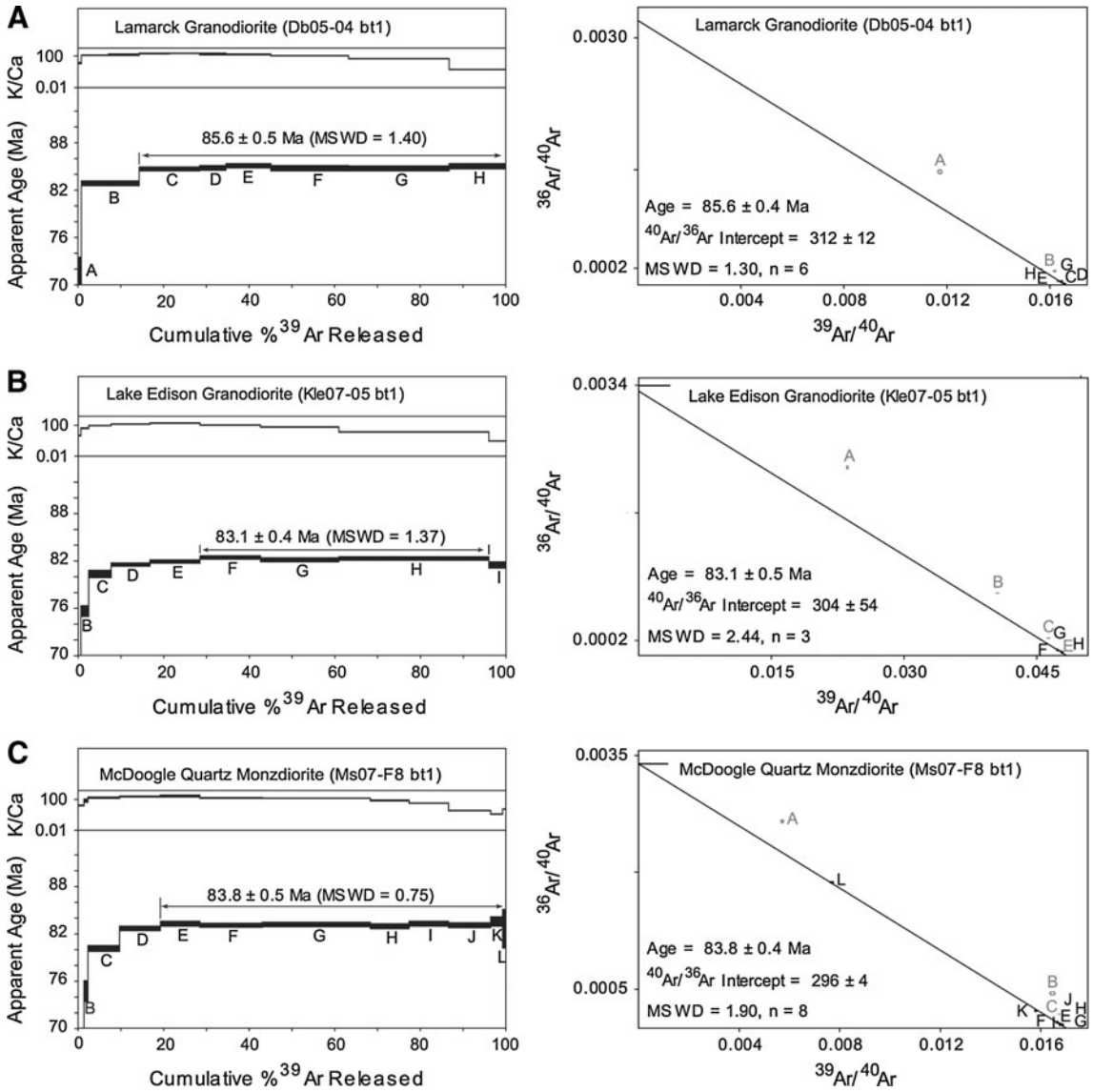

Fig. 6 Biotite $^{40}Ar/^{39}Ar$ step heating spectra and inverse isochrons from the John Muir Intrusive Suite. Argon ages are calculated using Fish Canyon standard age, $\lambda^{40}K_{\varepsilon}$ and $\lambda^{40}K_{\beta}$ of Renne et al. (2010). Errors incorporate analytical, J-value, ^{40}K decay constant, and Fish Canyon standard age uncertainties. Errors are reported at 2-sigma uncertainty. *Gray* heating steps on inverse isochron are excluded from regressions and age calculations (see text for "Discussion"). The *horizontal line* on inverse isochrons indicates $^{40}Ar/^{36}Ar = 295.5$

the range of zircon ages from the sample. Schaltegger et al. (2009) suggest using the youngest zircon fraction's age as a proxy for the crystallization age when a sample exhibits a protracted zircon growth history. Consequently, we use an age of 83.5 Ma for the crystallization age of sample Km07-06. The same interpretation may be valid for both the McDoogle Quartz Monzodiorite (Ms07-F8; Fig. 4) and the second Mono Creek Granite sample (Mc-1; Fig. 4) but is not distinguishable from the resorption/regrowth hypothesis.

Incremental emplacement

Zircon U–Pb crystallization ages indicate that the Muir suite assembled over about 12 Ma from 96 to 84 Ma (Fig. 4). Within the suite, individual plutons also record extended age ranges: combining the results from this study with those published by Coleman et al. (1995) requires that the Lamarck Granodiorite was assembled over at least 3 Ma, and data for the Mono Creek Granite suggest up to about 4 Ma for its assembly. Plutons with crystallization ages spanning millions of years and intrusive suites with age ranges approaching 12 Ma cannot be intruded as one (or just a few) pulses of magma but must have been assembled incrementally (Coleman et al. 2004; Glazner et al. 2004; Matzel et al. 2006). This is consistent with field data from the Muir suite and elsewhere, which require amalgamation of even texturally homogeneous plutons as incrementally assembled sheeted bodies (Mahan et al. 2003; Bartley et al. 2008;

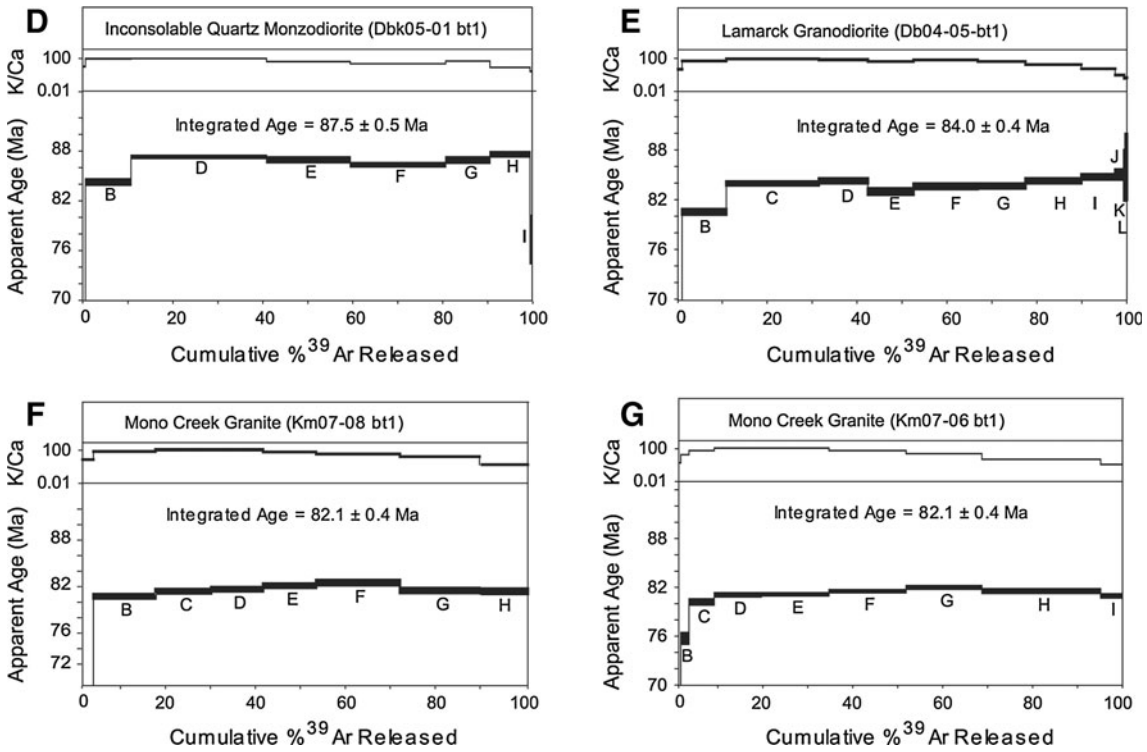

Fig. 6 continued

Stearns and Bartley 2010). Even the relatively rapidly assembled Torres del Paine pluton preserves evidence for incremental assembly (Michel et al. 2008). The growing body of data requiring million year age spans for the crystallization of plutons, supported by a growing body of field evidence for incremental assembly, suggests that incremental pluton growth is the norm and not the exception. Therefore, caution should be exercised when accepting a single age as representative of any pluton. Additionally, interpretation of the timing of structures by dating deformed or cross cutting plutons must be restricted to samples immediately adjacent to the structure of interest.

Interpretation of thermal histories

Zircon crystallization ages are concordant (within uncertainty) with titanite and hornblende ages for all samples in this study, thereby indicating rapid cooling to approximately 550°C immediately following intrusion. In addition, this suggests that the hornblende ages were not reset by younger intrusions in the suites. Following the initial interval of rapid cooling immediately after intrusion, slow cooling persisted for millions of years as indicated by the 2–11 Ma separation between hornblende and biotite ages (Fig. 7). Together, the data suggest that temperatures remained between hornblende and biotite closure temperatures for millions of years following intrusion.

Two interpretations can account for rapid, followed by slow, cooling: exhumation occurring millions of years after emplacement, or cooling complicated by multiple reheating events during the approximately 12 Ma intrusive history of the rocks.

During the time of emplacement, if ambient temperatures were above biotite closure, the protracted cooling through biotite closure temperatures could reflect cooling during exhumation. In this case, biotite ages would be set once rocks were exhumed through the biotite closure temperature isotherm. In the absence of folding or faulting, biotite ages reflecting regional exhumation cooling should fall in a narrow range (e.g., Renne et al. 1993). The spread of biotite ages throughout the Muir suite is inconsistent with this view (Fig. 7). Although the spread in ages could be the result of deformation yielding exhumation of some areas prior to others, no such deformation is evident in the region. Therefore, exhumation cooling is not favored as a mechanism producing the T-t histories throughout the Muir suite.

Thermal modeling shows that when plutons are assembled incrementally, as demonstrated for the Muir suite, temperatures oscillate with the intrusion and cooling of each magma pulse and remain above ambient background for extended time periods (Annen et al. 2006). Thus, the gap between hornblende and biotite ages for the Muir suite could reflect temperature oscillations associated with multiple

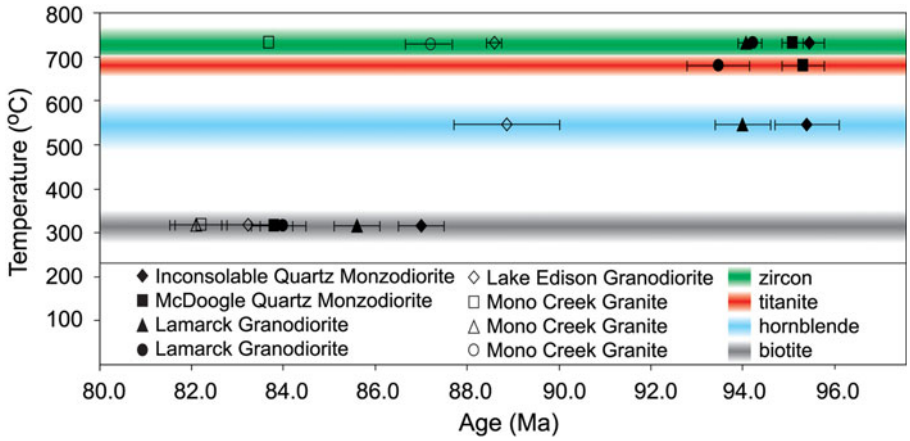

Fig. 7 Temperature-time (T-t) histories from plutons of the John Muir Intrusive Suite indicating initial rapid cooling through titanite and hornblende closure followed by protracted cooling through biotite closure. *Color shading* indicates the following: estimated zircon saturation temperatures (Watson and Harrison 1983) of 750–700°C, estimated titanite closure temperatures (700–660°C) after Scott and St-Onge (1995), estimated hornblende (580–490°C) and biotite (345–280°C) closure temperatures after Harrison (1981) and Harrison et al. (1985), respectively. Errors are reported at 2-sigma uncertainty except for one Mono Creek Granite zircon sample for which only an approximate age is given (see text for "Discussion")

intrusions of magma. The range of temperature oscillations appears to be limited to being between biotite and hornblende closure because K-feldspar multiple-diffusion-domain modeling suggests a distinct time gap between biotite closure (estimated to be 345–280°C) and feldspar cooling (models typically suggest temperatures of approximately 320°C; Davis 2010). If temperatures during incremental assembly were dropping significantly below 320°C, and biotite was getting reset during a subsequent heating event, high-temperature ages for the K-feldspar should be similar to the biotite ages. Instead the data suggest very slow cooling between biotite closure and the onset of high-temperature Ar retention in the K-feldspar (Davis 2010).

Throughout the Muir suite, the data indicate that there is a greater time gap between crystallization and subsequent passage through biotite closure for older plutons than for younger plutons (Fig. 8). Older plutons such as the Inconsolable Quartz Monzodiorite, McDoogle Quartz Monzodiorite, and Lamarck Granodiorite record an approximate 11–8 Ma gap; whereas, younger plutons such as the Lake Edison Granodiorite and Mono Creek Granite record an approximate 6–2 Ma gap between crystallization and biotite closure. Resetting of biotite dates in the oldest plutons by intrusion of the youngest plutons seems unlikely because they are separated by nearly 80 km. Instead, more protracted cooling in older plutons is consistent with modeling that shows the thermal anomalies of younger intrusions building across the decaying temperature profiles of older intrusions (e.g., Barton and Hanson 1989; Hanson and Barton 1989). Temperatures in the younger units likely did not stay elevated as long because the regional magmatic activity waned shortly after they intruded (e.g., Chen and Moore 1982). The regular SW to NE progression in the biotite ages mirrors the zircon age progression; therefore, we interpret the biotite ages to record the time–space progression of the end of magmatism.

Incremental emplacement and volcanic-plutonic connections

Detailed geochronology for the Lamarck Granodiorite and field mapping permit the calculation of an average magma flux during pluton growth. Estimating a thickness between 5–10 km using data from near-by plutons (McNulty et al. 2000; Hirt 2007) and an area of 600 km^2 (Bateman 1992), a long-term average magma flux between 0.001–0.002 $km^3\ a^{-1}$ is needed to construct the Lamarck Granodiorite. Expanding to the entire Muir suite, an estimated area of 1,700 km^2 (Bateman 1992) and a thickness between 5–10 km yields a slightly slower flux. These fluxes are consistent with those calculated for other plutons including the Tuolumne Intrusive Suite and the Mount Stuart batholith (Annen 2009) and the Mount Whitney Intrusive Suite (Davis 2010).

A growing body of geochronological data and numerical models show that the rate of magma emplacement is an important variable controlling whether a caldera-forming eruption is possible (Jellinek and DePaolo 2003; Glazner et al. 2004; Annen 2007, 2009; Crowley et al. 2007; Costa 2008). Numerical simulations show that magma fluxes greater than 0.1 $km^3\ a^{-1}$ are necessary to develop and maintain magma chambers voluminous enough to feed large (>400 km^3) ignimbrite eruptions (Annen 2009). Rapid magma fluxes are consistent with geochronologic

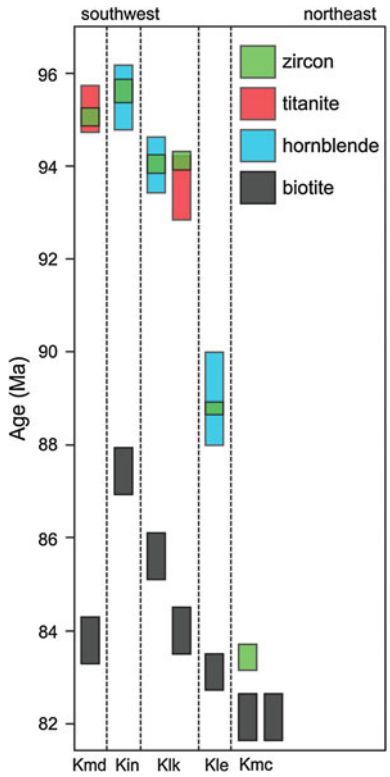

Fig. 8 Summary of geo-thermochronology data from samples of the John Muir Intrusive Suite for which both U–Pb and Ar ages are determined. Errors are reported at 2-sigma uncertainty, and data are arranged roughly from southwest (*left*) to northeast (*right*). Note that as the crystallization ages of the plutons get younger, the time interval between zircon and biotite ages decreases. Kmd, McDoogle Quartz Monzodiorite; Kin, Inconsolable Quartz Monzodiorite; Klk, Lamarck Granodiorite; Kle, Lake Edison Granodiorite; Kmc, Mono Creek Granite

data from ignimbrites that suggest magma residence times less than 1 Ma and likely less than 500 ka prior to eruption (Schmitz and Bowring 2001; Bachmann et al. 2007; Crowley et al. 2007; Costa 2008; Simon et al. 2008). Recent calculations that assume rapid pluton assembly times (10^3–10^5 years) suggest that growth rates of magma bodies on the order of 0.1 to >1 km^3 a^{-1} are necessary to support ignimbrite eruptions (de Silva and Gosnold 2007). However, no detailed geochronology for plutonic rocks supports such rapid assembly rates. In contrast, a growing number of geochronological studies indicate that pluton emplacement fluxes are orders of magnitude too low to develop large magma chambers (Glazner et al. 2004; Matzel et al. 2006; Michel et al. 2008). Finally, Jellinek and DePaolo (2003) predict the preferential storage of magma as plutons (rather than eruption) in large, thermally mature bodies for which the magma flux is low.

The low magma fluxes during assembly of the Lamarck Granodiorite and the Muir suite likely precluded the development of large, dominantly liquid magma chambers during construction. Modeling by Annen (2009) suggests that such low fluxes are capable of maintaining a magma chamber with only a few percent melt. This conclusion is consistent with geophysical data from active volcanic regions that never indicate the presence of significant melt percentages (>50%) in sub-volcanic magma chambers (Iyer 1984; Moran et al. 1999; Masturyono et al. 2001; Chu et al. 2010). If large magma chambers typically do not develop during pluton construction, then the genetic relationship hypothesized to exist between zoned plutons and zoned ignimbrites is problematic and must be reevaluated (e.g., Hildreth 2004; Bachmann et al. 2007; Lipman 2007).

Several lines of evidence suggest that the link between plutonic and volcanic rocks may not be through huge ignimbrite eruptions but rather through more typical arc magmatism. Data from the Chilean Andes indicates that volcanic centers record eruptive histories comparable to the assembly time for zoned intrusive suites (e.g., Aucanquilcha 10 Ma; Grunder et al. 2008; Walker et al. 2010). These centers are also similar in size to the zoned intrusive suites (approximately 3,000 km^2) and show similar patterns of compositional evolution through time (Grunder et al. 2008). Finally, although it is difficult to compare time scales, estimates of modern fill rates beneath Andean volcanoes made using InSAR are on the order of 0.05 km^3 a^{-1} (Pritchard and Simons 2004). These rates are intermediate between estimates necessary for ignimbrite formation and estimates of pluton filling rates, but it seems likely that this short-term measurement overestimates long-term rates. Taken together, we hypothesize that "Sierran-type" zoned intrusive suites are actively forming beneath modern arc volcanoes and that suites such as the Muir hold information about typical arc magmatism, rather than large, zoned ignimbrite events.

Conclusions

Zircon U–Pb geochronology results indicate that the John Muir Intrusive Suite was assembled over at least 12 Ma from 96 and 84 Ma. Assembly over millions of years favors the development of the intrusive suite, and the individual plutons within it, as a series of incrementally emplaced intrusions. Bulk mineral thermochronology indicate complicated cooling histories that were typically rapid immediately following intrusion, followed by slow cooling as temperatures were maintained between hornblende and biotite closure throughout assembly of the Muir suite.

The high density of U–Pb zircon geochronology for rocks in the Muir suite permits reasonable estimates of long-term magma flux during assembly. Estimated pluton assembly rates for the Muir suite and one of its members,

the Lamarck Granodiorite, are on the order of 0.001–0.002 $km^3\ a^{-1}$, similar to independent estimates of assembly rates from elsewhere. Thermal modeling reveals that assembly of plutons at such slow rates results in a persistently low melt fraction present. Therefore, it is unlikely that the Muir suite or the Lamarck Granodiorite ever existed as large, high-melt fraction magma chambers. This result is consistent with geophysical data for magma zones beneath active arcs, but is sharply at odds with petrologic models that place heavy emphasis on processes in high melt-fraction shallow magma chambers, and the concept that zoned intrusive suites are genetically linked with large silicic ignimbrite eruptions.

Acknowledgments This research was supported by National Science Foundation grant EAR-0538129 awarded to Coleman and EAR-0538094 awarded to John Bartley (University of Utah). Additional funding was provided by Sigma Xi (J. Davis, J. Gracely), the Geological Society of America (J. Davis, M. Stearns), the White Mountain Research Station (J. Davis, J. Gracely, R. Gaschnig), the University of Utah Department of Geology and Geophysics (M. Stearns), and the Martin Fellowship and Charles S. Bartlett funds administered by the University of North Carolina at Chapel Hill (J. Davis, J. Gracely, R. Gaschnig). We would like to especially acknowledge Allen Glazner, John Bartley, Matt Heizler for reviewing this manuscript and providing thoughtful insight pertaining to the issues addressed here. Special thanks to Matt Heizler and Lisa Peters who provided technical support at the New Mexico Geochronology Research Laboratory, New Mexico Bureau of Geology. We thank Jon Blundy, Luca Caricchi, and an anonymous reviewer for thoughtful insights and comments regarding this manuscript. Logistical support from Kings Canyon Nation Park and the National Forest Service is greatly appreciated.

References

Ague JJ, Brimhall GH (1988) Magmatic arc asymmetry and distribution of anomalous plutonic belts in the batholiths of California: effects of assimilation, crustal thickness, and depth of crystallization. Geol Soc Am Bull 100:912–927

Annen C (2007) The growth of magma bodies by amalgamation of discrete sheet intrusions: Implications for the formation of magma chambers. Eos Trans AGU (program and abstracts)

Annen C (2009) From plutons to magma chambers: thermal constraints on the accumulation of eruptible silicic magma in the upper crust. Earth Planet Sci Lett 284:409–416

Annen C, Scaillet B, Sparks RSJ (2006) Thermal constraints of the emplacement rate of a large intrusive complex: the Manaslu Leucogranite, Nepal Himalaya. J Petrol 47:71–95

Bachmann O, Miller CF, de Silva SL (2007) The volcanic-plutonic connection as a stage for understanding crustal magmatism. J Volcanol Geotherm Res 167:1–23

Bartley JM, Coleman DS, Glazner AF (2008) Incremental emplacement of granitic plutons by magmatic crack-seal. In: Petford N, Sparks S (eds) Plutons and Batholiths (Wallace Pitcher Memorial Issue). Trans R Soc Edinb Earth Sci 97:383–396

Barton MD, Hanson RB (1989) Magmatism and the development of low-pressure metamorphic belts: Implications from the western United States and thermal modeling. Geol Soc Am Bull 101:1051–1065

Bateman PC (1965) Geologic map of the blackcap mountain quadrangle, Fresno County, California. US Geol Surv Rep GQ-0529

Bateman PC (1992) Plutonism in the central part of the Sierra Nevada batholith, California. US Geol Surv Prof Pap 1483

Bateman PC, Dodge FCW (1970) Variations of major chemical constituents across the central Sierra Nevada batholith. Geol Soc Am Bull 81:409–420

Bateman PC, Moore JG (1965) Geologic map of the mount Goddard quadrangle, Fresno and Inyo counties, California. US Geol Surv Rep GQ-0429

Bateman PC, Carman MF, Clark LC, Jackson ED, Parker RL (1964) Geologic Map of the Big Pine 15-minute quadrangle, California

Bateman PC, Pakiser LC, Kane MF (1965) Geology and tungsten mineralization of the Bishop District California. US Geol Surv Prof Pap 470

Berger GW (1975) $^{40}Ar/^{39}Ar$ step heating of thermally overprinted biotite, hornblende and potassium feldspar from Eldora, Colorado. Earth Planet Sci Lett 26:387–408

Boudreau A, McBirney AR (1997) The Skaergaard layered series; part III, non-dynamic layering. J Pet 38:1003–1020

Chen JH, Moore JG (1982) Uranium-lead isotopic ages from the Sierra Nevada batholith, California. J Geophys Res 87B:4761–4784

Chu R, Helmberger DV, Sun D, Jackson JM, Zhu L (2010) Mushy magma beneath Yellowstone. Geophys Res Lett 37: LO1306

Coleman DS, Glazner AF (1998) The Sierra Crest magmatic event; rapid formation of juvenile crust during the Late Cretaceous in California. In: Ernst WG, Nelson CA (eds) Integrated earth and environmental evolution of the Southwestern United States; the Clarence A. Hall Jr. volume. Bellwether Publishing, USA, pp 253–272

Coleman DS, Glazner AF, Miller JS, Bradford KJ, Frost TP, Joye JL, Bachl CA (1995) Exposure of a Late Cretaceous layered mafic-felsic magma system in the central Sierra Nevada batholith, California. Contrib Mineral Petrol 120:129–136

Coleman DS, Gray W, Glazner AF (2004) Rethinking the emplacement and evolution of zoned plutons: Geochronologic evidence for incremental assembly of the Tuolumne Intrusive Suite, California. Geology 32:433–436

Costa F (2008) Residence times of silicic magmas associated with calderas. In: Gottsmann J, Martí J (eds) Developments in Volcanology 10. Caldera Volcanism: analysis, modeling, and response. Elsevier, pp 1–55

Crowley JL, Schoene B, Bowring SA (2007) U-Pb dating of zircon in the Bishop Tuff at the millennial scale. Geology 35:1123–1126

Davis JW (2010) Thermochronology and cooling histories of plutons: implications for incremental pluton assembly. PhD Dissertation, University of North Carolina at Chapel Hill

de Silva SL, Gosnold WD (2007) Episodic construction of batholiths: insights from the spatiotemporal development of an ignimbrite flare-up. J Volcanol Geotherm Res 167:320–335

Dodson MH (1973) Closure temperature in cooling geochronological and petrological systems. Contrib Mineral Petrol 40:259–274

Frost TP, Mahood GA (1987) Field, chemical, and physical constraints on mafic-felsic magma interaction in the Lamarck Granodiorite, Sierra Nevada, California. Geol Soc Am Bull 99:272–291

Frost TP, Mattinson JM (1988) Late Cretaceous U-Pb age of a mafic intrusion from the eastern Sierra Nevada, California. Isochron West 51:15–18

Frost TP, Mattinson JM (1993) Age and tectonic implications of mid-Mesozoic calc-alkalic hornblende-rich mafic plutonic rocks of the eastern Sierra Nevada, California. Isochron West 59:11–16

Gaschnig RM (2005) Cause, timing, and significance of brittle deformation in Little Lakes Valley, eastern Sierra Nevada,

California. MS Thesis, University of North Carolina at Chapel Hill

Glazner AF, Bartley JM, Coleman DS, Gray W, Taylor RZ (2004) Are plutons assembled over millions of years by amalgamation from small magma chambers? Geol Soc Am Today 14:4–11

Gracely JT (2006) Rapid pluton emplacement via multiple discrete processes, Lamarck Granodiorite, Central Sierra Nevada, California. MS Thesis, University of North Carolina at Chapel Hill

Grunder AL, Klemetti EW, Feeley TC, Cm McKee (2008) Eleven million years of arc volcanism at the Aucanquilcha Volcanic Cluster, northern Chilean Andes: implications for the life span and emplacement of plutons. Trans R Soc Edinb Earth Sci 97:415–436

Hanson RB, Barton MD (1989) Thermal development of low-pressure metamorphic belts: results from two-dimensional numerical models. J Geophys Res 94:10363–10377

Harrison TM (1981) Diffusion of ^{40}Ar in hornblende. Contrib Mineral Petrol 78:324–331

Harrison TM, Duncan I, McDougall I (1985) Diffusion of ^{40}Ar in biotite: temperature, pressure, and compositional effects. Geochim Cosmochim Acta 49:2461–2468

Hathaway M (2002) Geology of the inconsolable range, east-central Sierra Nevada, kings Canyon National Park and John Muir Wilderness, California; magmatic emplacement and the dynamic evolution of composite intrusions. PhD Dissertation, University of California at Los Angeles

Heizler MT, Lux DR, Decker ER (1988) The age and cooling history of the Chain of Ponds and Big Island Pond plutons and the Spider Lake Granite, west-central Maine and Quebec. Am J Sci 288:925–952

Hildreth W (2004) Volcanological perspectives on long Valley, Mammoth Mountain, and Mono Craters: several contiguous but discrete systems. J Volcanol Geotherm Res 136:169–198

Hirt WH (2007) Petrology of the Mount Whitney Intrusive Suite, eastern Sierra Nevada, California: implications for the emplacement and differentiation of the composite felsic intrusion. Geol Soc Am Bull 119:1185–1200

Iyer HM (1984) Geophysical evidence for the locations, shapes and sizes, and internal structures of magma chambers beneath regions of quaternary volcanism. Philo Trans R Soc Lond Math Phys Sci 310:473–510

Jaffey AH, Flynn KF, Glendenin LE, Bentley WC, Essling AM (1971) Precision measurement of half-lives and specific activities of ^{235}U and ^{238}U. Phys Rev C4:1889–1906

Jellinek AM, DePaolo DJ (2003) A model for the origin of large silicic magma chambers: precursors of caldera-forming eruptions. Bull Volcanol 65:363–381

Kistler RW (1990) Two different lithosphere types in the Sierra Nevada, California. In: Anderson JL (ed) The nature and origin of Cordilleran magmatism. Geol Soc Am Mem 174:271–281

Kistler RW, Chappell BW, Peck BL, Bateman PC (1986) Isotopic variation in the Tuolumne intrusive suite, central Sierra Nevada, California. Contrib Mineral Petrol 94:205–220

Krogh TE (1973) A low-contamination method for hydrothermal decomposition of zircon and extraction of U and Pb for isotopic age determinations. Geochim Cosmochim Acta 37:485–494

Lipman PW (2007) Incremental assembly and prolonged consolidation of Cordilleran magma chambers: evidence from the Southern Rocky Mountain volcanic field. Geosphere 3:42–70

Lo C, Onstott TC (1989) ^{39}Ar recoil artifacts in chloritized biotite. Geochim Cosmochim Acta 53:2697–2711

Lockwood JP, Lydon PA (1975) Geologic map of the Mount Abbot quadrangle, central Sierra Nevada, California. US Geol Sur Rep GQ-1155

Ludwig KR (1980) Calculation of uncertainties of U-Pb isotope data. Earth Planet Sci Lett 46:212–220

Ludwig KR (1998) On the treatment of concordant uranium-lead ages. Geochim Cosmochim Acta 62:665–676

Ludwig KR (2003) Isoplot 3.00; A geochronological toolkit for Microsoft Excel. Berkley Geochronology Center Spec Pub 4

Mahan KH, Bartley JM, Coleman DS, Glazner AF, Carl BS (2003) Sheeted intrusion of the synkinematic McDoogle pluton, Sierra Nevada, California. Geol Soc Am Bull 115:1570–1582

Masturyono, McCaffrey R, Wark DA, Roecker SW, Fauzi, Ibrahim G, Sukhyar (2001) Distribution of magma beneath the Toba caldera complex, north Sumatra, Indonesia, constrained by three-dimensional P wave velocities, seismicity, and gravity data. Geochem Geophy Geosys 2000GC000096

Mattinson JM (2005) Zircon U-Pb chemical abrasion ("CA-TIMS") method: combining annealing and multi-step partial dissolution analysis for improved precision and accuracy of zircon ages. Chem Geol 220:47–66

Matzel JEP, Bowring SA, Miller RB (2006) Time scales of pluton construction at differing crustal levels: examples from the Mount Stuart and Tenpeak intrusions, North Cascades, Washington. Geol Soc Am Bull 118:1412–1430

McBirney AR (1995) Mechanisms of differentiation in the Skaergaard Intrusion. J Geol Soc Lond 152:421–435

McBirney AR, Nicolas A (1996) The Skaergaard layered series; part II, magmatic flow and dynamic layering. J Pet 38:569–580

McNulty BA, Tobisch OT, Cruden AR, Gilder S (2000) Multistage emplacement of the Mount Givens pluton, central Sierra Nevada batholith, California. Geol Soc Am Bull 112:119–135

Michel J, Baumgartner L, Putlitz B, Schaltegger U, Ovtcharova M (2008) Incremental growth of the Patagonian Torres del Paine laccolith over 90 k.y. Geology 36:459–462

Miller JS, Wooden JL (2004) Residence, resorption, and recycling of zircons in Devils Kitchen Rhyolite, Coso Volcanic Field, California. J Petrol 45:2155–2170

Miller WM, Fallick AE, Leake BE, Macintyre RM, Jenkin GRT (1991) Fluid disturbed hornblende K-Ar ages from the Dalradian rocks of Connemara, Western Ireland. J Geol Soc Lond 148:985–992

Miller JS, Matzel JEP, Miller CF, Burgess SD, Miller RB (2007) Zircon growth and recycling during the assembly of large, composite arc plutons. J Volcanol Geotherm Res 167:282–299

Moore JG (1963) Geology of the Mount Pinchot quadrangle, southern Sierra Nevada, California. US Geol Surv Bull 1130

Moran SC, Lees JM, Malone SD (1999) P wave crustal velocity structure in the greater Mount Rainier area from local earthquake tomography. J Geophys Res 104:10775–10786

Mundil R, Ludwig KR, Metcalfe I, Renne PR (2004) Age and timing of the Permian mass extinctions: U/Pb dating of closed-system zircons. Science 305:1760–1763

Parrish RP (1987) An improved micro-capsule for zircon dissolution in U-Pb geochronology. Chem Geol 66:99–102

Parrish RP, Krogh TE (1987) Synthesis and purification of ^{205}Pb for U-Pb geochronology. Chem Geol 66:103–110

Pritchard ME, Simons M (2004) An InSAR-based survey of volcanic deformation in the southern Andes. Geophys Res Lett 31:1–4

Renne PR (2006) Progress and challenges in K-Ar and ^{40}Ar/^{39}Ar geochronology. In: Olszewski T (ed) Geochronology: emerging opportunities. Paleont Soc Pap 12:47–66

Renne PR, Tobisch OT, Saleeby JB (1993) Thermochronologic record of pluton emplacement, deformation, and exhumation at Courtright shear zone, central Sierra Nevada, California. Geology 21:331–334

Renne PR, Swisher CC, Deino AL, Karner DB, Owens TL, DePaolo DJ (1998) Intercalibration of standards, absolute ages and uncertainties in ^{40}Ar/^{39}Ar dating. Chem Geol 145:117–152

Renne PR, Mundil R, Balco G, Min K, Ludwig KR (2010) Joint determination of ^{40}K decay constants and ^{40}Ar*/^{40}K for the Fish

Canyon sanidine standard and improved accuracy for $^{40}Ar/^{39}Ar$ geochronology. Geochim Cosmochim Acta 74:5349–5367

Saleeby J, Kistler RW, Longiaru S, Moore JG, Nokleberg WJ (1990) Middle Cretaceous silicic metavolcanic rocks in the Kings Canyon area, central Sierra Nevada, California. In: Anderson JL (ed) The nature and origin of the Cordilleran magmatism. Geol Soc Am Mem 174:251–270

Saleeby J, Ducea MN, Busby C, Nadin E, Wetmore PH (2008) Chronology of pluton emplacement and regional deformation in the southern Sierra Nevada batholith, California. In: Wright JE, Shervais JW (eds) Ophiolites, Arcs, and Batholiths. Geol Soc Am Spec Pap 438:1–31

Sanders RE, Heizler MT, Goodwin LB (2006) $^{40}Ar/^{39}Ar$ thermochronology constraints on the timing of Proterozoic basement exhumation and fault ancestry, southern Sangre de Cristo Range, New Mexico. Geol Soc Am Bull 118:1489–1506

Schaltegger U, Brack P, Ovtcharova M, Peytcheva I, Schoene B, Stracke A, Marocchi M, Bargossi GM (2009) Zircon and titanite recording 1.5 million years of magma accretion, crystallization and initial cooling in a composite pluton (southern Adamello batholith, northern Italy). Earth Planet Sci Lett 286:208–218

Schmitz MD (2010) Boise state isotope geology laboratory LABSHARE. http://earth.boisestate.edu/isotope/labshare.html

Schmitz MD, Bowring SA (2001) U-Pb zircon and titanite systematics of the Fish Canyon Tuff: an assessment of high precision U-Pb geochronology and its application to young volcanic rocks. Geochim Cosmochim Acta 65:2571–2587

Scott DJ, St-Onge MR (1995) Constraints on Pb closure temperature in titanite based rocks from Ungava Orogen, Canada: implications for U-Pb geochronology and P-T-t path determinations. Geology 23:1123–1126

Simon JI, Renne PR, Mundil R (2008) Implications of pre-eruptive magmatic histories of zircons for U-Pb geochronology of silicic extrusions. Earth Planet Sci Lett 266:182–194

Singer BS, Pringle MS (1996) Age and duration of the Matuyama-Brunhes geomagnetic polarity reversal from $^{40}Ar/^{39}Ar$ incremental heating analyses of lavas. Earth Planet Sci Lett 139: 47–61

Sisson VB, Onstott T (1986) Dating blueschist metamorphism: a combined $^{40}Ar/^{39}Ar$ and electron microprobe approach. Geochim Cosmochim Acta 50:2111–2117

Stacey JS, Kramers JD (1975) Approximation of terrestrial lead isotope evolution by a two stage model. Earth Planet Sci Lett 26:207–221

Stearns MA, Bartley JM (2010) Refinement of the crack-seal model: insights from the McDoogle pluton, Sierra Nevada, CA. Geol Soc Am Bull (submitted)

Steiger RH, Jäger E (1977) Subcommission on geochronology; convention on the use of decay constants in geo- and cosmochemistry. Earth Planet Sci Lett 36:359–362

Stern TW, Bateman PC, Morgan BA, Newell MF, Peck DL (1981) Isotopic U-Pb ages of zircon from granitoids of the central Sierra Nevada, California. US Geol Surv Prof Pap 1185:1–17

Taylor JR (1982) An introduction to error analysis: the study of uncertainties in physical measurements. University Science Books, California

Tera F, Wasserburg GJ (1972) U-Th-Pb systematics in three Apollo 14 basalts and the problem of initial Pb in lunar rocks. Earth Planet Sci Lett 14:281–304

Tikoff B, Saint Blanquat M (1997) Transpressional shearing and strike-slip partitioning in the Late Cretaceous Sierra Nevada magmatic arc, California. Tecton 16:442–459

Tikoff B, Teyssier C (1992) Crustal-scale, en echelon "P-shear" tensional bridges: a possible solution to the batholithic room problem. Geology 20:927–930

Tobisch OT, Saleeby JB, Renne PR, McNulty B, Tong W (1995) Variations in deformation fields during development of a large-volume magmatic arc, central Sierra Nevada, California. Geol Soc Am Bull 107:148–166

Waite GP, Moran SC (2009) Vp structure of Mount St. Helens, Washington, USA, imaged with local earthquake tomography. J Volcanol Geotherm Res 182:113–122

Walker BA, Grunder Al, Wooden JL (2010) Organization and thermal maturation of long-lived arc systems: evidence from zircons at the Aucanquilcha volcanic cluster, northern Chile. Geology 38:1007–1010

Wartho J (1995) Apparent argon diffusive loss $^{40}Ar/^{39}Ar$ age spectra in amphiboles. Earth Planet Sci Lett 134:393–407

Wartho J, Dodson MH, Rex DC, Guise PG (1991) Mechanisms of Ar release from Himalayan metamorphic hornblende. Am Mineral 76:1446–1448

Watson EB, Harrison TM (1983) Zircon saturation revisited: temperature and composition effects in a variety of crustal magma types. Earth Planet Sci Lett 64:295–304